Electronic Supplementary Material (ESI) for Lab on a Chip.

Supplemental Material for "Acoustofluidic Medium Exchange for Preparation of Electrocompetent Bacteria using channel wall trapping"

M. S. Gerlt, P. Ruppen, M. Leuthner, S. Panke, and J. Dual*

E-mail: dual@imes.mavt.ethz.ch

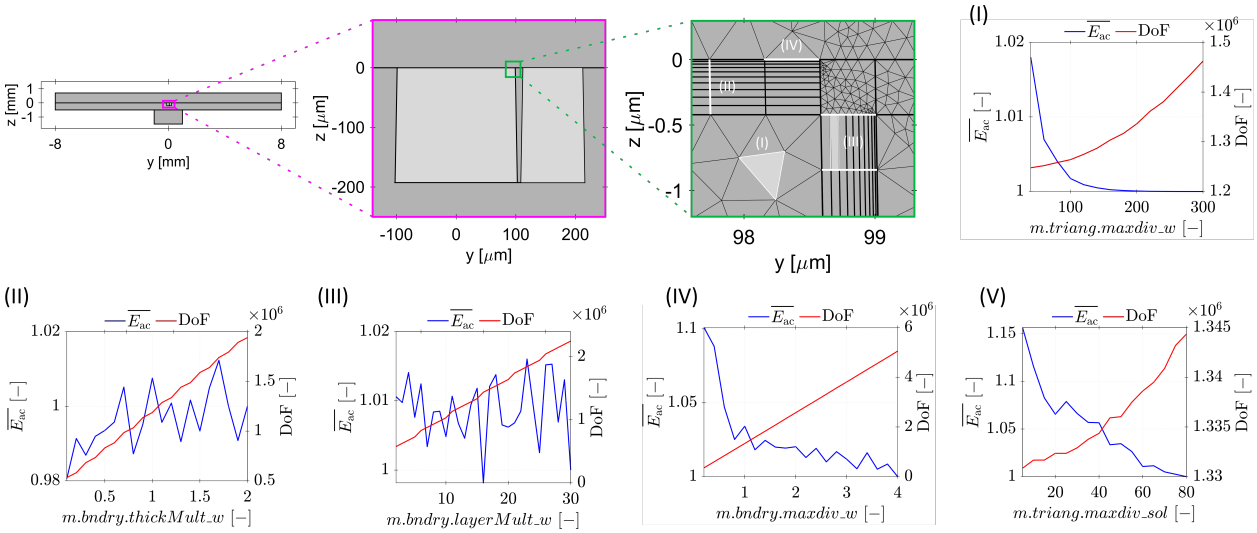

Figure ESI 1: : Mesh study of the COMSOL Model. We introduced five mesh parameters reflecting different aspects of the mesh. (I) Maximal longitudinal element size on the mesh junctions. (II) length of the mesh refinement layer, generated for the viscous boundary layer. (III) The number of rows within the mesh refinement layer. (IV) width of the elements in the mesh refinement layer. (V) maximal element size throughout the whole mesh. As long as the mesh refinement layer is set higher than the viscous boundary layer, it does not influence the overall quality of the mesh. With $\tilde{E_{ac}}$ as the average energy density in the water channel and DoF the number of degrees of freedom. We chose the following mesh parameters for all simulations in this work, corresponding to an error below 1% in respect to the finest mesh: (I) 200, (II) 1, (III) 15, (IV) 1.2, (V) 50.

Supplemental Material

Numerical Model

We used the Solid Mechanics interface to model the solid components of the model (silicon, glass, piezoelectric element). To account for damping, we modelled the glass as a linear elastic material with complex Lamé parameters. The silicon was modeled as an anisotropic linear elastic material with its elasticity matrix. The piezoelectric element was modeled with a Piezoelectric Material model. Finally, a thin eleastic layer was introduced at the interface between the piezoelectric element and silicon to model the glue layer (spring constant per unit area). Please refer to table ESI 1 for all material parameters used in the numerical model.

To account for the piezoelectric effect, the Electrostatics interface was applied to the piezo-

Table ESI 1: Table of the material properties and damping factors.

Parameter	Symbol and value	Unit
Glass Pyrex[1]		
Density	$\rho^{\text{glass}} = 2240$	$[\text{kg m}^{-3}]$
Quality factor	$Q^{\text{glass}} = 2420$	$[\text{kg m}^{-3}]$
Lamé parameters	$\lambda = 23.1 \times 10^9(1 + i/Q^{\text{glass}})$	$[\text{N m}^{-2}]$
	$\mu = 24.1 \times 10^9(1 + i/Q^{\text{glass}})$	$[\text{N m}^{-2}]$
Silicon[2]		
Density	$\rho^{\text{silicon}} = 2240$	$[\text{kg m}^{-3}]$
Stiffness matrix	$c_{ij}^{\text{silicon}} = (1 + i0)C_{ij}, with$	
	$C_{11} = C_{22} = C_{33} = 166$	[GPa]
	$C_{12} = C_{13} = C_{23} = 64$	[GPa]
	$C_{44} = C_{55} = C_{66} = 80$	[GPa]
Piezo Pz26[3]		
Density	$\rho^{\text{piezo}} = 7700$	$[\text{kg m}^{-3}]$
Electric damping	$tan\delta = 0.003$	[–]
Quality factor	$Q^{\text{piezo}} = 100$	[–]
Stiffness matrix	$c_{ij}^{\text{piezo}} = 0.965(1 + i/Q^{\text{piezo}})C_{ij}, with$	
	$C_{11} = C_{22} = 155, C_{12} = 94.1$	[GPa]
	$C_{13} = C_{23} = 79.9, C_{33} = 110$	[GPa]
	$C_{44} = C_{55} = C_{66} = 27.3$	[GPa]
Coupling matrix	$e_{ij}^{\text{piezo}} = (1 + i(1/(2Q^{\text{piezo}}) - tan\delta/2))E_{ij}, with$	
	$E_{31} = E_{32} = -5.48, E_{33} = 13.6$	$[\text{C m}^{-2}]$
	$E_{24} = E_{15} = 9.55$	$[\text{C m}^{-2}]$
Permittivity tensor	$\epsilon_{ij}^{\text{piezo}} = (1 - i(tan\delta))\mathcal{E}_{ij}, with$	
	$\mathcal{E}_{11} = \mathcal{E}_{22} = 929, \mathcal{E}_{33} = 518$	$[\text{C m}^{-2}]$
Glue layer H20E[4]		
Quality factor	$Q^{\text{glue}} = 10$	[–]
Spring constants	$k_{11} = 2.06(1 + i/Q^{\text{glue}})/5 \times 10^{-6}$	$[\text{N m}^{-2}]$
	$k_{22} = 8.94(1 + i/Q^{\text{glue}})/5 \times 10^{-6}$	$[\text{N m}^{-2}]$

electric element. Charge conservation was implemented for the whole domain and an electric potential of 40 V was applied to one side of the piezoelectric element. Subsequently, the Solid Mechanics interface and the Electrostatics interface were coupled by the Piezoelectric Effect interface.

The Thermoviscous Acoustics interface was applied to both channels. The materials inside both channels were modeled with the standard material parameters provided by the software.

The Thermoviscous Acoustic-Structure Boundary interface was implemented to couple the

Solid Mechanics interface and the Thermoviscous Acoustics interface at the water-silicon and the air-silicon interfaces.

To incorporate the acoustic streaming in our simulations, we extended the procedure described in,[5] where they used the limiting velocity approach. We followed,[6] resolving the streaming in the boundary layer together with accounting for the Stokes drift. The Creeping Flow interface was assigned to the water domain. Source terms were enforced through Volume Forces across the domain. Finally, the second-order pressure field was constrained by setting a Pressure Point Constraint to zero at an arbitrary point of the domain.

Python script for control of experimental setup

We wrote a Python script that communicates with the pressure pump and the wave generator. We used the programming interface provided by the supplier (LineUP Series SDK, Fluigent) for communication with the pressure pumps and flow rate sensors. We used a self-written Python library to communicate with the wave generator (the library for the AFG-2225 wave generator can be found on GitLab: **https://git.bsse.ethz.ch/pruppen/afg2225-library**).

Electroporator - time constant and conductivity

During the electric pulse, a $10\mu F$ capacitor is discharged, creating an exponentially declining voltage with time constant τ . Inside the electroporator, a 600Ω resistor is placed in parallel with the sample cuvette along with a 30Ω resistor in series with the sample cuvette.[7] The time constant, that is displayed on the electroporator screen is thus a function of the sample conductivity, as indicated in the following equation:

$$R = \frac{600\Omega(30\Omega + R_s)}{630\Omega + R_s}, \tag{1}$$

$$\tau = CR, \tag{2}$$

with the equivalent resistance of the resistor circuit R, the sample resistance R_s and the micropulser capacitance C.

Control Experiment - Centrifugation Medium Exchange

We conducted an additional control experiment for a better comparison of our method with the standard method for preparation of electrocompetent cells - centrifugation. We grew cells the same way as described in section 3.3. The culture was divided into three 8 mL samples and centrifugation and subsequent transformation was performed in triplicates. The samples were centrifuged at 4000 g for 10 minutes, the supernatant was removed and the cells were then resuspended in 8mL of ultrapure water. This step was repeated three times for each sample. The samples before and after centrifugation were diluted and plated on non-selective agar plates and the colonies counted after overnight incubation at $37°C$. Counting of the CFU the next day showed a recovery of $48 \pm 13\%$ of the cells after the three centrifugation and resuspension steps, which is close to the 47% recovery obtained with our device. Again, only viable (colony forming) cells are counted. Afterwards, plasmid was added, transformation was performed and plating occured in the same way as described in section 3.7 for the sample from the acoustic medium exchange. $13 \pm 1\%$ of the initial cells were successfully transformed.

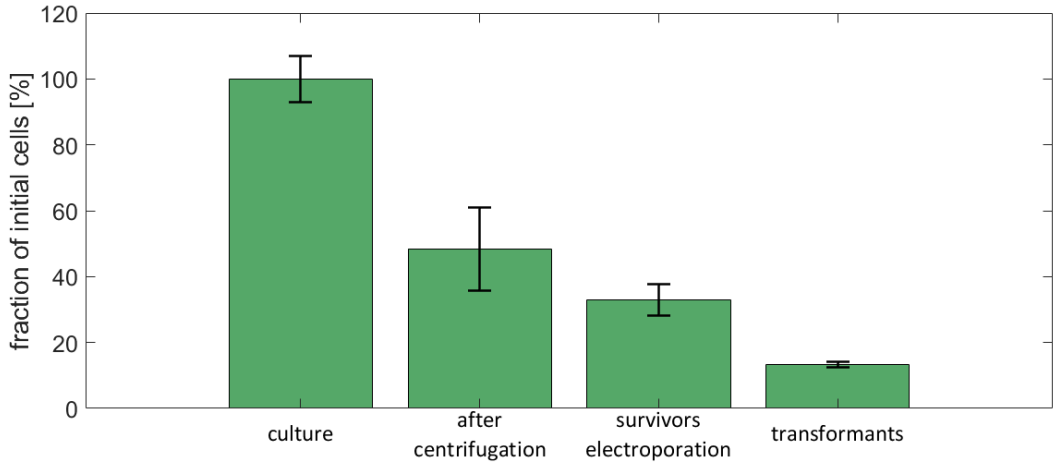

Figure ESI 2: : Preparation of electrocompetent cells using centrifugation. culture: starting cell concentration before electroporation. Plated on LB Agar. after electroporation: competent cells prepared by 3x centrifugation and resuspension in ultrapure water. Plated on LB Agar. survivors electroporation: cells after electroporation with $2.0\,\mathrm{ng\,\mu L^{-1}}$ pUC19 plasmid and one hour recovery in SOC medium. Plated on LB Agar. transformants: cells after electroporation with $2.0\,\mathrm{ng\,\mu L^{-1}}$ pUC19 plasmid and one hour recovery in SOC medium. Plated on LB Agar + $50\,\mathrm{\mu g\,mL^{-1}}$ carbenicilin.

References

(1) Selfridge, A. Approximate Material Properties in Isotropic Materials. *IEEE Transactions on Sonics and Ultrasonics* **1985**, *32*, 381–394.

(2) Hopcroft, M. A.; Nix, W. D.; Kenny, T. W. What is the Youngs Modulus of Silicon? *Journal of Microelectromechanical Systems* **2010**, *19*, 229–238.

(3) MeggittFerroperm, Properties of Pz26. *https://www.meggittferroperm.com* **accessed: 2021-05-21**,

(4) Epotek, properties of H20E. *https://www.epotek.com/* **accessed: 2021-05-21**,

(5) Muller, P. B.; Barnkob, R.; Jensen, M. J. H.; Bruus, H. A numerical study of microparticle acoustophoresis driven by acoustic radiation forces and streaming-induced drag forces. *Lab on a Chip* **2012**, *12*, 4617–4627.

(6) Baasch, T.; Pavlic, A.; Dual, J. Acoustic radiation force acting on a heavy particle in

a standing wave can be dominated by the acoustic microstreaming. *Physical Review E* **2019**, *100*, 061102.

(7) MicroPulser ™ Electroporation Apparatus Operating Instructions and Applications Guide. Bio-Rad.